This is an open access article published under an ACS AuthorChoice License, which permits copying and redistribution of the article or any adaptations for non-commercial purposes.

ACS chemical biology

Letters

pubs.acs.org/acschemicalbiology

Protein Sialylation Regulates a Gene Expression Signature that Promotes Breast Cancer Cell Pathogenicity

Rebecca A. Kohnz,[†] Lindsay S. Roberts,[†] David DeTomaso,[‡] Lara Bideyan,[†] Peter Yan,[†] Sourav Bandyopadhyay,[§,∥] Andrei Goga,[§,∥] Nir Yosef,[‡] and Daniel K. Nomura*[,†]

[†]Departments of Chemistry, Molecular and Cell Biology, and Nutritional Sciences and Toxicology, University of California, Berkeley, Berkeley, California 94720, United States

[‡]Department of Electrical Engineering and Computer Science, University of California, Berkeley, Berkeley, California 94720, United States

[§]Division of Hematology/Oncology, Department of Cell and Tissue Biology, University of California, San Francisco, 513 Parnassus Avenue HSW616, San Francisco, California 94143, United States

[∥]University of California, San Francisco Helen Diller Family Comprehensive Cancer Center, Box 0128, San Francisco, California 94143, United States

Supporting Information

ABSTRACT: Many mechanisms have been proposed for how heightened aerobic glycolytic metabolism fuels cancer pathogenicity, but there are still many unexplored pathways. Here, we have performed metabolomic profiling to map glucose incorporation into metabolic pathways upon transformation of mammary epithelial cells by 11 commonly mutated human oncogenes. We show that transformation of mammary epithelial cells by oncogenic stimuli commonly shunts glucose-derived carbons into synthesis of sialic acid, a hexosamine pathway metabolite that is converted to CMP-sialic acid by cytidine monophosphate *N*-acetylneuraminic acid synthase (CMAS) as a precursor to glycoprotein and glycolipid sialylation. We show that CMAS knockdown leads to elevations in intracellular sialic acid levels, a depletion of cellular sialylation, and alterations in the expression of many cancer-relevant genes to impair breast cancer pathogenicity. Our study reveals the heretofore unrecognized role of sialic acid metabolism and protein sialylation in regulating the expression of genes that maintain breast cancer pathogenicity.

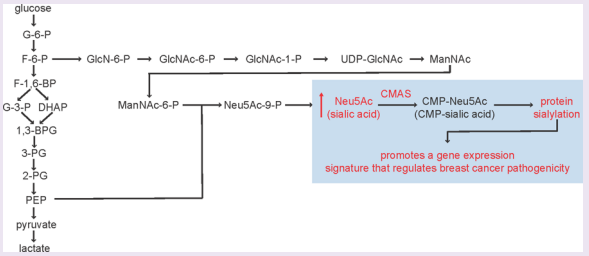

Cancer cells possess fundamentally altered metabolism that fuels their pathogenicity, including an addiction to heightened aerobic glycolytic metabolism also known as the "Warburg effect". Many mechanisms have been discovered for how altered glycolytic metabolism fuels tumorigenesis, including the use of glycolytic carbons for synthesis of macromolecular precursors such as amino acids, nucleic acids, and fatty acids for generating proteins, DNA, and membranes for rapid cell proliferation, but there are likely yet unexplored pathways that link the Warburg effect to cancer pathogenicity.[1−3]

To identify metabolic pathways that may be heightened in breast cancer, we profiled common changes in isotopic [^{13}C]glucose carbon incorporation into metabolic pathways upon oncogenic transformation of MCF10A mammary epithelial cells using 11 individual commonly mutated or amplified human oncogenes (Figure 1A; Table S1). This model uses isogenically derived cells, enabling not only direct identification of metabolic changes conferred by specific oncogenes but also metabolic alterations more broadly shared by transformation across many oncogenic lesions.[4] We sought to identify potential metabolic nodes that may be commonly heightened in breast cancer cells that could be subsequently investigated for their importance to breast cancer pathogenicity.

Our isotopic-labeling-based metabolomic profiling showed that glycolytic carbon incorporation was particularly and commonly heightened for specific metabolites, including citrate, fumarate, malate, and oxaloacetate from the tricarboxylic acid (TCA) cycle as well as sialic acid from the hexosamine pathway (Figure 1A−C; Figure S1, Table S1). Heightened glycolytic metabolism into the TCA cycle has been well-studied in the context of generating carbon sources for macromolecular building blocks to enable cell proliferation and generation of metabolites that influence transcriptional and signaling pathways to drive cancer pathogenicity.[1] However, the role of sialic acid and the hexosamine pathway in cancer are not as well understood. We thus focused our efforts toward elucidating the role of sialic acid metabolism in breast cancer cell pathogenicity.

Sialic acids are primarily synthesized *de novo* and, upon metabolic activation, are incorporated at the terminal positions

Received: May 18, 2016
Accepted: July 5, 2016

 © XXXX American Chemical Society

DOI: 10.1021/acschembio.6b00433
ACS Chem. Biol. XXXX, XXX, XXX−XXX

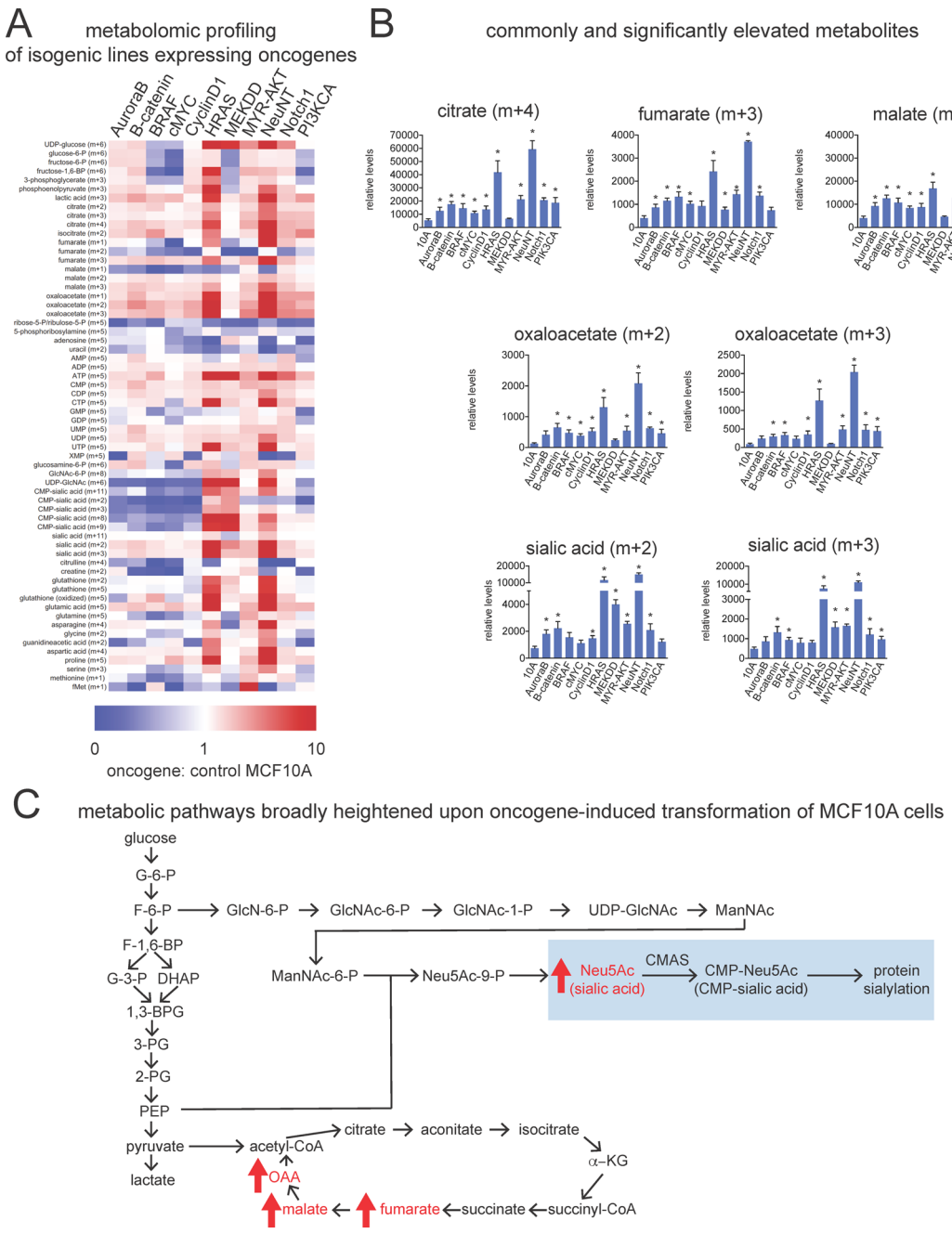

Figure 1. Isotopic tracing of [^{13}C]glucose into metabolic pathways in an isogenic panel of MCF10A mammary epithelial cells individually expressing 11 oncogenes. (A) Relative levels of [^{13}C] metabolites from [U−^{13}C]glucose labeling (24 h) of MCF10A control cells or MCF10A cells stably expressing one of 11 commonly mutated or amplified oncogenes in cancer. Metabolites were measured using a targeted SRM-based approach. Notations in parentheses indicate the number of isotopes incorporated into each individual metabolite from [^{13}C]glucose. Red and blue colors represent heightened or reduced [^{13}C] incorporation into metabolites compared to MCF10A control cells. (B) Bar graphs showing relative levels of [^{13}C] metabolites from (A) for those metabolites showing significantly heightened [^{13}C] incorporation compared to MCF10A controls in eight or more oncogenes. (C) The metabolites in (B) placed within metabolic pathway maps. Data in (B) are presented as mean ± SEM, n = 3−5/group. Significance is presented as *p < 0.05 compared to MCF10A control cells. Raw data for this study is presented in Table S1.

of both N- and O-linked glycan chains. Sialic acid must be activated to cytidine monophosphate (CMP)-sialic acid by cytidine monophosphate *N*-acetylneuraminic acid synthase (CMAS) before sialylation of glycoproteins or glycolipids can occur. We note that the levels of [^{13}C]CMP-sialic acid are not as universally heightened upon oncogenic transformation as seen with [^{13}C]sialic acid (Figure S1). This may be due to increased flux of this metabolite into proteins or gangliosides or possibly reduced formation of this metabolite. Nonetheless, our results showing heightened [^{13}C]sialic acid levels suggested that these cells may be amplifying glycolytic flux into the hexosamine pathway potentially leading to heightened sialylation of proteins, prompting us to investigate the role of sialylation in breast cancer pathogenicity. Sialylation is an important post-translational modification on glycosylated cell-surface proteins, and these sialoglycoproteins are known to be enriched on the cell surface of cancer cells to drive cancer malignancy.[5]

DOI: 10.1021/acschembio.6b00433
ACS Chem. Biol. XXXX, XXX, XXX−XXX

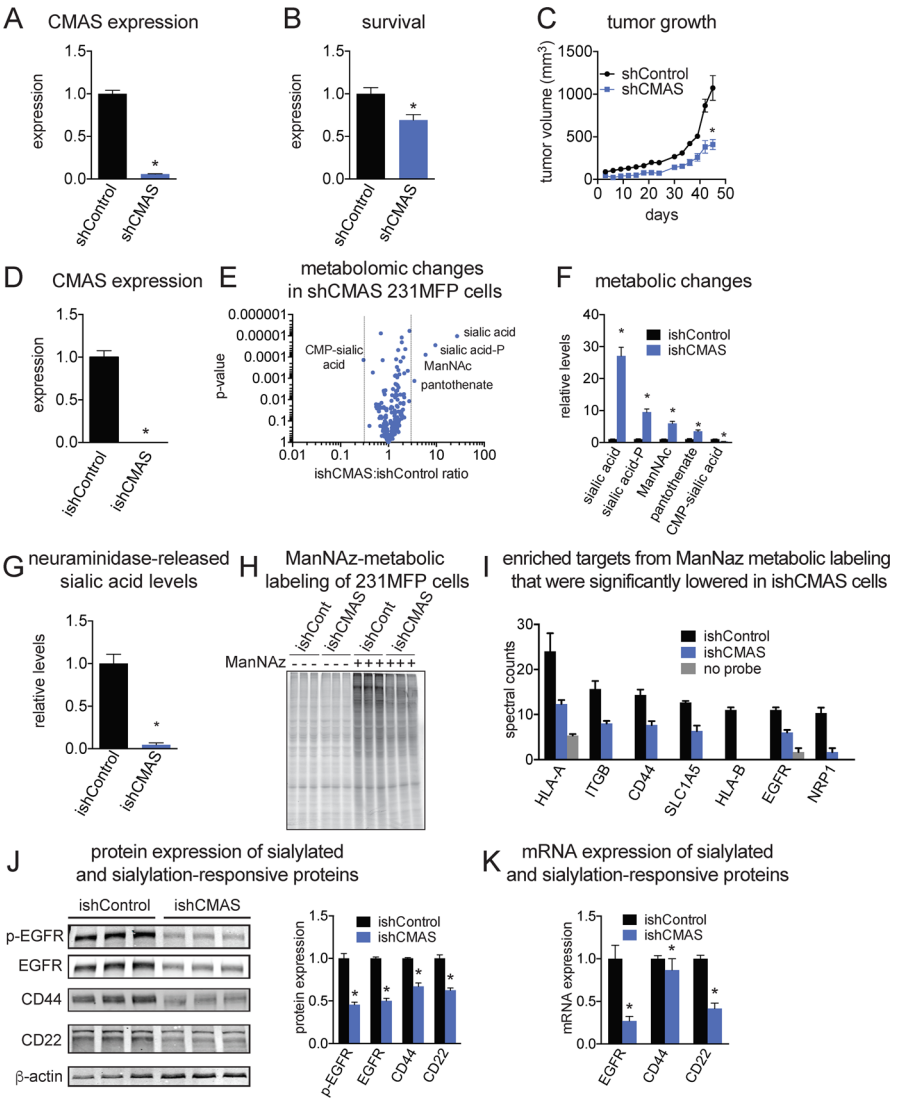

Figure 2. Knockdown of CMAS in 231MFP breast cancer cells. (A) CMAS was constitutively knocked down using RNA interference. CMAS expression was determined in shControl and shCMAS 231MFP cells by RT-qPCR. (B) Serum-free cell survival in shControl and shCMAS 231MFP cells 48 h after seeding. (C) Tumor xenograft growth of shControl and shCMAS 231MFP cells in immune-deficient mice. (D) Induction of hairpin expression targeting CMAS for 5 d using doxycycline (ishCMAS) and CMAS expression was determined by RT-qPCR in ishControl and ishCMAS 231MFP cells. (E) Targeted metabolomic profiling of ishControl and ishCMAS 231MFP cells. Full data is shown in Table S2. (F) Levels of metabolites significantly changing in ishCMAS cells compared to ishControl 231MFP cells >2-fold with a $p < 0.01$. (G) Neuraminidase-released sialic acid levels quantified by SRM-based targeted LC-MS/MS. (H) ManNAz treatment of ishControl and ishCMAS 231MFP cells and fluorescent detection of sialoglycoproteins. Rhodamine-alkyne was coupled to metabolically labeled proteins by click-chemistry, and proteins were separated by SDS/PAGE and visualized by in-gel fluorescence. (I) ManNAz treatment of ishControl and ishCMAS 231MFP cells and proteomic identification of sialoglycoproteins. Biotin-alkyne was coupled to metabolically labeled proteins by click-chemistry, and proteins were avidin-enriched, tryptically digested, and analyzed by nanoLC-MS/MS. No-probe refers negative control, in which cells were not treated with ManNAz. Raw data are shown in Table S3. (J) Protein expression of phospho-EGFR, total EGFR, CD44, CD22, and β-actin were quantified by densitometry. (K) mRNA expression levels of EGFR, CD44, and CD22 determined by qPCR. Data in (A–D, F, G, I, J, and K) are presented as mean ± SEM, n = 3–8/group. Significance is presented as $^*p < 0.05$ compared to shControl or ishControl cells.

To investigate the role of sialylation and the enzyme CMAS in breast cancer cells, we knocked down the expression of CMAS in the estrogen receptor/progesterone receptor/HER2 receptor-negative (triple-negative) human breast cancer 231MFP cell line using RNA interference using a short-hairpin oligonucleotide (shCMAS) (Figure 2A). While there are many sialyltransferases responsible for adding sialic acids onto glycan chains, only CMAS can bioactivate the cellular pool of sialic acid and thus provide sialyltransferases with substrates for sialylation. Modulation of CMAS expression could therefore be used as a tool for investigating the effect of reduced protein sialylation on breast cancer pathogenicity. We show that CMAS knockdown in 231MFP cells impaired prolonged serum-free cell survival and tumor xenograft growth in immune-deficient mice, indicating that CMAS expression and sialylation capacity was important in maintaining breast cancer pathogenicity (Figure 2B–C).

We next performed single-reaction monitoring (SRM)-based targeted LC-MS/MS metabolomic profiling to investigate the metabolic and biochemical alterations conferred by CMAS knockdown in 231MFP cells (Figure 2D,E; Table S2). We filtered for changes in metabolite levels that were highly

DOI: 10.1021/acschembio.6b00433
ACS Chem. Biol. XXXX, XXX, XXX–XXX

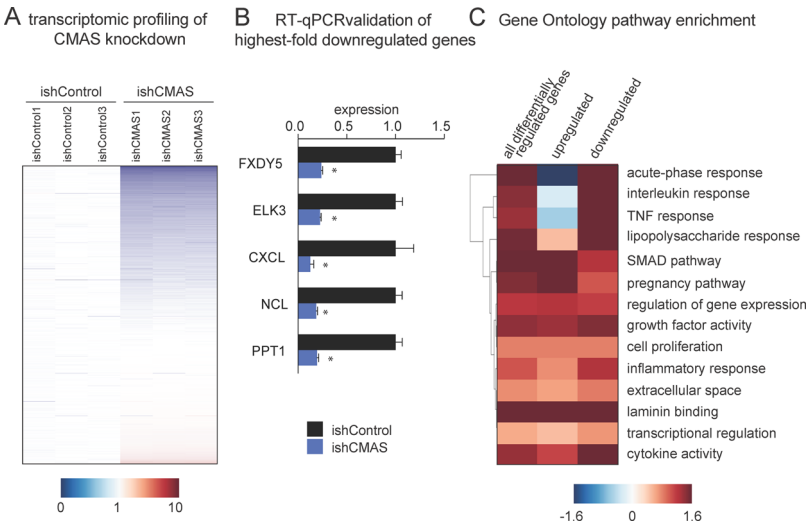

Figure 3. Transcriptional changes conferred by CMAS knockdown. (A) Transcriptomic data from ishControl and ishCMAS 231MFP cells from RNA sequencing profiling. Blue and red colors denote down- and upregulation of transcript levels, respectively. White denotes no change. Raw data is shown in Table S4. (B) Validation of highest-fold transcriptomic changes from RNA sequencing by RT-qPCR. (C) Gene ontology pathway analysis of differentially expressed genes ($p < 0.01$). Highly differential pathways here indicate pathways significantly enriched ($p < 0.01$ and false-discovery rate adjusted) with >2-fold change. Shading in the plot represents $\log_2$ of the ratio of overlap between differential genes and gene ontology gene set compared to expected overlap by chance. Enrichment of pathways are shown by all differentially regulated genes (both up or downregulated) as well as genes within pathways that were up or downregulated. Genes within selected pathways enriched are shown in Figure S3. Data in (B) are presented as mean ± SEM, $n = 3$/group. Significance is presented as $^*p < 0.05$ compared to ishControl cells.

significant ($p < 0.01$) and robustly changing (>5-fold) in shCMAS cells compared to shControl cells. CMAS knockdown led to impressive greater than 20-fold elevations in the intracellular free sialic acid pool. Additionally, we observed other hexosamine pathway metabolites increasing, with >5-fold changes in *N*-acetylneuraminic acid-9-phosphate and *N*-acetylmannosamine (ManNAc). The only significantly altered metabolite not found in the hexosamine pathway was an increase in pantothenate (vitamin B_5), a necessary metabolite for coenzyme A synthesis. While the exact role for pantothenate metabolism in the context of sialic acid synthesis is unclear, we predict that increased sialic acid production would similarly need an increased substrate pool of acetyl-CoA. Conversely, we observed a reduction in the product of the reaction catalyzed by CMAS, CMP-sialic acid, with a 5-fold decrease in shCMAS cells as compared to control cells. Taken together, our data indicate that CMAS knockdown specifically causes a large accumulation of intracellular sialic acid which then causes a backlog of hexosamine pathway intermediates and depletes the cells of CMP-sialic acid (Figure 2F). Importantly, CMAS knockdown creates a unique and distinct metabolic profile that does not appear to affect other pathways such as glycolysis, TCA cycle, or the synthesis of amino acids or nucleotides.

We next assessed whether CMAS knockdown caused changes in the amount of sialic acids capping terminal glycan chains. We removed freely soluble intracellular metabolites including sialic acid via solvent extraction, followed by enzymatic digestion with neuraminidase to cleave off sialic acid from glycan chains. Following SRM-based LC-MS/MS analysis of enzymatically released sialic acid, we found that CMAS knockdown caused a drastic reduction in the total amount of sialic acid-capped glycans (Figure 2G).

To determine whether this CMAS knockdown impaired the ability of the cell to sialylate newly synthesized or post-translationally modified proteins due to the lack of CMP-sialic acid, we labeled cells with a bioorthogonal azide-modified mannosamine (ManNAz). ManNAz is utilized by cells in a manner similar to ManNAc, converted biochemically into an azide-modified sialic acid, and then metabolically incorporated into nascent glycans to create an azido-sialoglycan.[6] Upon using copper-catalyzed click-chemistry to append a rhodamine handle for gel-based fluorescent detection of sialylated proteins, we showed that CMAS knockdown reduced the incorporation of azide-modified sialic acid into glycoproteins. This labeling strategy showed that *de novo* sialylation of glycoproteins is reduced with CMAS knockdown (Figure 2H).

We next wanted to further characterize the identification of sialylated glycoproteins in 231MFP cells that were affected by CMAS knockdown. We thus labeled shControl and shCMAS 231MFP cells with ManNAz, appended a biotin handle via click-chemistry for subsequent avidin enrichment, tryptic digestion, and proteomic analysis. We identified 7 proteins that were both significantly enriched with ManNAz labeling compared to DMSO-treated cells (>4-fold), as well as significantly reduced in shCMAS cells compared to shControl cells (Figure 2I, Table S3). Interestingly, these sialylated proteins included important oncogenic signaling proteins such as epidermal growth factor receptor (EGFR) as well as the breast cancer stem cell marker CD44. We further validated EGFR as a sialylated protein through biotin-mediated enrichment of azide-tagged sialylated EGFR followed by immunoblotting with a total EGFR antibody (Figure S2).

To further elucidate whether loss of sialylation mediated by CMAS knockdown affected EGFR signaling, we measured EGFR expression and activity. We observed an approximate 50% reduction of phosphotyrosine[1068] EGFR level in shCMAS cells compared to shControl cells (Figure 2J). However, we were surprised to also observe an equivalent reduction in total EGFR protein expression. The ratio of phosphorylated EGFR to total EGFR total protein level was unchanged with CMAS knockdown, indicating that reduced levels of phosphorylated EGFR were likely due to downregulation of EGFR protein

DOI: 10.1021/acschembio.6b00433
ACS Chem. Biol. XXXX, XXX, XXX−XXX

expression. Similarly, we also observed reductions in the protein levels of all glycosylated forms of CD44 with CMAS knockdown (Figure 2J). Although not found through our ManNAz screen, we report here that the Siglec sialic-acid-binding family member CD22 is also downregulated with CMAS knockdown (Figure 2J). CD22 is known to bind sialic-acid-containing glycan ligands not just *in trans* but also on the same cell surface, suggesting that there may be a potential feedback loop between autonomous cellular display of sialoglycans and protein expression of CD22.[7,8]

We initially considered the possibility that reduced sialylation of glycoproteins led to their post-translational downregulation in protein expression via increased lysosomal or proteasomal degradation (Figure S3). This was not the case, since lysosomal inhibition by chloroquine or proteosomal inhibition by MG132 did not rescue the EGFR downregulation conferred by CMAS knockdown (Figure S3). We instead found that EGFR, CD44, and CD22 are transcriptionally downregulated in shCMAS cells to an extent that is comparable to their respective protein levels (Figure 2K). Collectively, our data indicate that CMAS knockdown and impaired protein sialylation leads to impaired cancer pathogenicity, potentially through the transcriptional downregulation of cell-surface sialylated or sialic-acid responsive proteins including EGFR, CD44, and CD22.

Intrigued by these results, we next performed transcriptomic analysis using RNASeq to investigate additional transcriptional changes that occur upon loss of CMAS expression and globally reduced cellular sialylation. Interestingly, over the 40 000 mRNA transcripts profiled, we observed 221 transcripts changing significantly greater than 2-fold ($p < 0.05$ with multiple-testing correction for statistical analysis) with expression level (as read by transcripts per kilobase million) of >30 (Figure 3A; Table S4). Incredibly, of these 221 transcripts that change with CMAS knockdown, we observe a substantial overlap with our ManNAz metabolic labeling proteomics data. HLA-A, HLA-B, EGFR, NRP1, and SLC1A5 are all sialylated according to our proteomic identification and are transcriptionally downregulated with decreased cellular sialylation capacity. We were particularly interested in additional genes that may be downregulated by CMAS knockdown to better understand the scope of transcriptional regulation controlled by cellular sialylation pathways. Among the strongest downregulated (>4-fold) transcriptional alterations in shCMAS cells included palmitoyl protein thioesterase 1 (PPT1), nucleolin (NCL), chemokine C-X-C motif ligand 1 (CXCL1), ETS-domain protein (ELK3), dysadherin (FXDY5) (Figure 3B), which were subsequently validated by RT-qPCR. Notably, all of these genes separately have been previously demonstrated to be important mediators of cancer pathogenicity. For example, PPT1 inhibition has been shown to increase cell death in neuroblastoma cell lines, whereas PPT1 overexpression protects these cells against apoptosis.[9,10] Nucleolin (NCL) is a plasma membrane protein that is highly expressed in several types of cancers and NCL antagonists triggers autophagic cell death in glioblastoma cells and impairs tumor growth.[11,12] Chemokine C-X-C Motif Ligand 1 (CXCL1) is a chemokine that has been shown to play a major role in inflammation, angiogenesis, tumorigenesis, and metastasis through regulating NF-κB signaling.[13] ETS-domain protein (ELK3) inhibition has been shown to reduce breast cancer cell migration, invasiveness, and metalloprotease expression.[14] High dysadherin (FXYD5) expression is correlated with metastasis and poor prognosis of many cancer types, and FXYD5 has been shown to promote motility and survival in breast cancer cells through AKT signaling.[15]

We also performed gene ontology analyses to identify molecular functions, cellular components, and biological process pathways that were enriched on the basis of the differentially expressed genes (Figure 3B; Figure S4). We see abundant transcriptional alterations in genes encoding transmembrane and secreted proteins, which is perhaps related to the known glycosylation of nearly all proteins of these types. We observe transcriptional changes in many secreted proteins including growth factors important in cancer, such as TGF-beta.[16] Most strikingly, however, among the biological processes that were significantly altered upon CMAS knockdown were those involved in immunological responses (Figure 3C; Figure S4). It has become clear with recent studies in cancer immunology that chemokines and their receptors play complex biological roles in host−tumor interactions, including cell survival and metastatic potential. Differential sialylation can alter activity of receptors and change cellular response to ligand secretion.[17−19] Here we observe transcriptional downregulation of cytokines interleukin 1 and 6 (IL-1, IL-6), both of which are commonly upregulated in breast cancer.[20−22] We see downregulation of many chemokine ligands such as CXCL2 and 10, CCL2 and 20, and the promiscuous chemokine receptor CCR1. Chemokines and their receptors have numerous implications in cancer, particularly in immune cell infiltration of tumors and influence of metastatic or site-specific spread of tumor cells.[23] Taken together, our results indicate that cellular sialylation broadly regulates transcription of inflammatory and secretory pathways that are necessary for aggressive cellular phenotypes, and reduction in cellular sialylation capacity disrupts breast cancer pathogenic features.

Here we show that CMAS knockdown in 231MFP breast cancer cells causes broad transcriptional changes resulting in the downregulation of many genes that are important in maintaining cancer cell pathogenicity. We report that oncogenic transformation of mammary epithelial cells by multiple different commonly mutated or amplified human oncogenes resulted in heightened glucose incorporation into sialic acid, an important metabolite used for glycan sialylation. Our results are consistent with previous studies that have shown that transformation of cancer cells by KRAS or other oncogenic programs, such as epithelial-to-mesenchymal transition, leads to stimulation of glycolytic metabolism into hexosamine biosynthesis.[24,25] Our data indicates that, unknown until now, many other oncogenic programs also contribute to diversion of glycolytic intermediates toward the hexosamine pathway. Sialic acid has been previously shown to be involved in resistance to apoptotic signaling, immune cell evasion, chemotherapeutic resistance, cancer progression, and metastasis. Sialyltransferases and sialidases are also known to be dysregulated in cancers; inhibition of protein sialylation through knockdown of individual sialyltransferases has been shown to impair cancer pathogenicity, but the mechanism underlying these changes have remained unclear.[5,26]

Here, we show that globally impairing protein sialylation by knockdown of CMAS leads to impaired phenotypic hallmarks of breast cancer pathogenicity and moreover results in broad negative alterations in gene expression of several key transformation and malignancy-promoting genes, including the glycoproteins EGFR and CD44, as well as downregulation of a host of other genes with known involvement in cancer progression. Whether the loss of cellular sialylation can

DOI: 10.1021/acschembio.6b00433
ACS Chem. Biol. XXXX, XXX, XXX−XXX

additionally alter the glycosylation pattern of individual proteins, impacting their function or regulation, is yet to be determined. While we show that CMAS knockdown leads to striking biochemical changes in the hexosamine pathway metabolites, we believe that the phenotypes and transcriptional changes observed are likely due to reduced sialylation.

We do not yet understand by which mechanism(s) CMAS knockdown leads to the noted transcriptional changes or the extent of the contribution of these transcriptional changes to the observed phenotypes. There is a precedent for transcriptional changes conferred by modulation of other hexosamine metabolites. Wellen et al. showed that glucose deprivation led to marked reduction in glutamine uptake and progressive cellular atrophy in mammalian cells through the *N*-acetylglucosamine (GlcNAc)-dependent downregulation of IL-3 receptor α, which in-turn led to transcriptional regulation of amino acid transporters.[27] In addition, O-GlcNAc modifications have also been shown to control transcriptional programs through modification of transcriptional complexes or epigenetic regulation.[28] Our data thus far point to indirect transcriptional regulation of many genes through impairing protein sialylation, including sialylated proteins EGFR and CD44, which are well-studied in the context of cancer. We postulate that reduced protein sialylation, perhaps of a particular yet unidentified protein, may lead to lysosomal or proteasome-mediated degradation and in turn cause the observed transcriptional signature we report here. Future studies would be necessary to identify such a protein, if any, by comparing protein abundance to gene expression to identify proteins that are downregulated only at the protein level.

Here we reveal a potential novel pathway through which heightened utilization of glucose through glycolysis effect fuels cancer pathogenicity via shunting metabolic intermediates into hexosamine biosynthesis of sialic acids. We show that heightened glycolytic metabolism generates increased sialic acid levels as a substrate for glycan sialylation, in turn maintaining a transcriptional signature rich in expression of genes involved in breast cancer cell pathogenicity. We further show that reducing cellular sialylation through knockdown of CMAS leads to transcriptional reprogramming and reduced breast cancer pathogenicity.

EXPERIMENTAL PROCEDURES

Cell Lines and Culture Conditions. 231MFP cells were generated from xenograft explants of MDA-MB-231 cells and were a gift from Benjamin Cravatt at The Scripps Research Institute. 231MFP cells were cultured in L15 media containing 10% fetal bovine serum, supplemented with 1% glutamine (200 mM stock), and grown at 37 °C in 0% CO_2. MCF10A and their derivative lines were from a previous study.[4,29] MCF10A and related lines were cultured in DMEM/F12K media containing 5% horse serum, supplemented with 1% glutamine (200 mM stock), 20 ng/mL EGF (Santa Cruz Biotechnology), 100 ng/mL cholera toxin (Sigma), 10 ng/mL insulin (Santa Cruz Biotechnology), and 500 ng/mL hydrocortisone (Sigma) and maintained at 37 °C at 5% CO_2. 293T/17 cells were purchased from ATCC and cultured in DMEM media containing 10% fetal bovine serum, supplemented with 1% glutamine (200 mM stock), and grown at 37 °C in 5% CO_2. Unless otherwise specified, all cell culture materials were purchased from Gibco. During lentivirus production and infection, all cell lines were switched to heat-inactivated serums in their respective media formulations and supplemented with hexadimethrine bromide (Sigma, 0.1% vol/vol of 10 mg mL^{-1} solution). For induction of shRNA expression, cells were stably transduced with pCMV-TetR-blast (Addgene) followed by transduction with shRNA constructs. Cells expressing TetR were maintained used tetracycline-free fetal bovine serum (Hyclone). Doubly transduced cells were incubated with doxycycline (Sigma, 5 μg/mL in DMSO) for the indicated time period. For most experiments, cells were harvested after 5 days of hairpin induction. Doxycline did not affect standard cell culture maintenance protocols such as trypsinization.

Generating CMAS Knockdown Cells. For stable and inducible RNA interference-mediated knockdown of CMAS expression, the short hairpin oligonucleotide sequence used was the following: CCGGTTCGACAGACCATGATGAAATCgtgtgctgtccGATTTCATCATGGTCTGTCGAATTTTTG. Lower-case letters designate a standard stem-loop structure. The oligonucleotide was cloned into pENTR/TER+ (Addgene) using Gateway BP Clonase II (Invitrogen) and then into pLenti-X1-puro (Addgene) using Gateway LR Clonase II (Invitrogen).

For inducible RNAi-mediated knockdown of CMAS expression, cell lines were created by stable expression of the tetracycline repressor protein driven under the CMV promoter (Addgene #716−1). The tetracycline-controlled transcriptional activation system used here for generating inducible CMAS knockdown is a method of inducible shRNA expression where transcription can be turned on in an inducible manner. Here, we transduced cells with the tetracycline receptor (TetR) that interacts with the Tet operator to repress shRNA expression until the addition of doxycycline, after which the shRNA can be expressed.[30]

CMAS hairpin sequences targeting the CDS and 5′UTR were chosen for *in vitro* validation and were ordered as HPLC-purified oligos from Elim Biosciences. Sequence of hairpins are as follows, given as 5′ to 3′, and supplemented with 5′ *Bgl*II overhang on the forward oligo and on the reverse oligo 3′ with a *Hin*dIII overhang (overhangs not shown). These oligos were cloned into pENTR/TER+ (Addgene #17338) using Gateway BP Clonase II (Invitrogen) and then into pLenti-X1-puro (Addgene #17297) using Gateway LR Clonase II (Invitrogen). Inducible expression of a hairpin targeting eGFP was used as a control. shControl: GATCCCGCAAGCTGACCCTGAAGTTCATGT gtgctgtccATGAACTTCAGGGTCAGCTTGCTTTTTGGAAA. TetR expressing was confirmed in stable cell lines expressing TetR by RT-qPCR (forward oligo: CGACGCCTTAGCCATTGAGA and reverse oligo: TTGCTCCATCGCGATGACTT) and displaying puromycin resistance to 10 μg/mL puromycin (Sigma).

Phenotypic Assays. Cellular survival assays were performed in 96-well plates with 20 000 cells/well. Live cells were fixed with formalin and stained with Hoechst 33342 dye (Invitrogen), and fluorescent signal was measured according to the manufacturer's procotol.

Western Blots and qPCR. Whole-cell lysate was collected by washing cells twice in cold PBS and lysed in freshly made buffer (containing the following: 20 mM Tris pH 7.5, 150 mM NaCl, 1 mM EDTA, 1 mM EGTA, 1% Triton X-100, 2.5 mM pyrophosphate, 50 mM NaF, 5 mM β-glycero-phosphate, 1 mM Na_3VO_4, 50 nM calyculin A (EMD Millipore), and protease inhibitors (Roche)). Lysate was incubated on a rotator at 4 °C for 30 min, and insoluble material was removed via centrifugation at 13 000 rpm for 10 min. SDS-PAGE analysis of proteins were performed using Bio-Rad mini or midi electrophoretic chambers and precast gels. Gels were transferred to nitrocellulose membranes. Membranes were washed in TBST, blocked in 5 wt %/vol dried nonfat milk in TBST, and incubated in primary antibodies overnight at 4 °C with shaking. Secondary antibodies were purchased from Rockland (antirabbit; catalog number 611-145-003) and used at 1:10 000 dilution in 5 wt %/vol dried nonfat milk in TBST at room temperature. Primary antibodies used in this study: Phospho-EGFR (catalog number 3777), EGFR (catalog number 4267), cyclophilin A (catalog number 2175), and beta actin (catalog number 4970) from Cell Signaling Technologies, and CD44 (catalog number ab51037) from Abcam from Sigma, and typically used at 1:1000 dilution in 5% BSA wt/vol in TBST.

RNA from cells was harvested using Trizol (Invitrogen) according to manufacturer's protocol. Synthesis of cDNA from total RNA was performed using Maxima reverse transcriptase (Thermo). Primers were ordered from Elim Biosciences and used in conjunction with 2X

DOI: 10.1021/acschembio.6b00433
ACS Chem. Biol. XXXX, XXX, XXX−XXX

SYBR master mix (Thermo) and a 3-step amplification repeating 40X on CFX96 thermocycler (Bio-Rad). Primers used are as follows: CMAS, F: ACCTGGCAGCCCTAATTCTG and R: TCGAAACCCATACACTCTGGAA. EGFR, F: TTGCCGCAAAGTGTGTAACG and R: GTCCTGTTTTCAGGCCAAGC. Cyclophilin A, F: CCCACCGTGTTCTTCGACATT and R: GGACCCGTATGCTTTAGGATGA. CXCL1, F: TCACAGTGTGTGGTCAACAT and R: AGCCCCTTTGTTCTAAGCCA. DHRS9, F: AAGGAAGAAGCCACTGTGCAT and R: GCTGTGGTGGGTCCAACTTC. SOAT1, F: TAGGATGCTCAGCCGGAGGT and R: CAACGTCGCCTGCTAAGCTA. RPIA, F: AGTGCTGGGAATTGGAAGTGG and R: GGGAATACAGACGAGGTTCAGA. ESM1, F: AGAATCTTAGCACAAACAGGACT and R: CAAAACCTAACAGCTTATGCAGC. NCEH1, F: GCAAGCCACTTCCCATCTCT and R: CCTTCGATGATGCAGGTGTC. TAGLN3, F: GAGAATCCGCGTTGCCTACT and R: AAGTTGAAGAGGAGAATTTTTGGC. PPT1, F: TGTTTTTGGACTCCCTCGATG and R: CATGCCAGTATTCGGCTTGC. NCL, F: GGTGGTCGTTTCCCCAACAAA and R: GCCAGGTGTGGTAACTGCT. ELK3, F: ATCTGCTGGACCTCGAACGA and R: TTCTGCCCGATCACCTTCTTG. FXYD5, F: GGTTATGCCGGAATCGTTGC and R: CTGTGTCTTCCCTCTCTGGC. CD44, F: CTGCCGCTTTGCAGGTGTA and R: CATTGTGGGCAAGGTGCTATT. CD22, F: GCACCCTGAAACCCTCTACG and R: ATCAAACTTCGAGGTGTTCTTGT. Whenever possible, primers were designed to amplify all transcriptional variants.

Tumor Xenograft Studies. Human cell line xenografts were established by transplantation of cancer cells ectopically into the right flank of female C.B17 SCID mice (Taconic Farms). Cells were washed with PBS, trypsinized, and harvested in serum-containing medium. After centrifugation, cells were washed twice with serum-free medium and placed into a suspension of 2.0×10^4 cells/mL, and 100 μL was injected per flank. Growth of the tumors was measured every 3 days with calipers.

ManNAz Labeling. 231MFP cells were treated with ManNAz or DMSO (Life Technologies, 25 μM final concentration) for 24 h in serum-containing media. Cells were rinsed three times with PBS to remove excess ManNAz, cells were scraped into cold PBS, pelleted by centrifuging at 3000 rpm for 3 min, lysed via sonication probe, and total protein was determined using Bradford reagent (Bio-Rad). Click-chemistry using rhodamine-alkyne (Life Technologies) or biotin-alkyne (Click Chemistry Tools) was performed using previously reported procedures.[31] Proteomics analysis was performed using a qExactive plus mass spectrometer.

Transcriptome Analysis. RNA was extracted from cells using a spin column preparation technique (Qiagen RNeasy Plus). Quality of RNA was assessed with a BioAnalyzer (Agilent) and scored a 10 out of 10 RIN. Library construction with pooling and sequencing was performed through the University of California, Davis RNA sequencing facility. RNA-seq reads were first trimmed using Trimmomatic to improve mappability.[32] Trimmed reads were aligned to the RefSeq hg38 transcriptome (GRCh38.2) by Bowtie2,[33] and RSEM[34] was used to estimate the abundance (expected read count and transcripts per million, TPM) of each gene. DESeq was used to compare the expected counts between control samples and sh496 knockouts and estimate fold changes and associated *p*-values (corrected for multiple-testing using the Benjamini and Hochberg procedure).[35,36] Several genes were quantified multiple times due to alternative isoforms unrelated by RefSeq annotation. Prior to DeSeq analysis, these count estimates were summed to produce a single count estimate per RefSeq gene symbol. Genes with less than 10 reads in total were removed at this stage. Analysis of the data can be found in Table S4.

Metabolomic Profiling. For metabolomic profiling, cell pellets (1×10^6 cells per replicate) were flash-frozen and subsequently extracted in 40:40:20 acetonitrile/methanol/water, with inclusion of 10 nM D_3-^{15}N-serine and 10 nM $^{13}C_2$-n-acetylneuraminic acid as internal standards for extraction efficiency. Insoluble debris was separated via centrifugation at 13 000 rpm for 10 min. For U−^{13}C-glucose tracing experiments, 5 mM (final concentration) labeled glucose (Cambridge Isotope Laboratories Inc.) or an equivalent of unlabeled glucose (Sigma-Aldrich) was added to glucose-free RPMI media (Gibco). Cells were incubated for a 24 h period at 37 °C at 5% CO_2 before pelleting and extraction. Ten microliters of this extracted supernatant was used for targeted SRM LC-MS/MS on an Agilent 6460 QQQ-LC/MS/MS. Separation of metabolites was achieved using normal-phase chromatography with a Luna 5 mm NH_2 column (Phenomenex) using a mobile phase (Buffer A, acetonitrile) followed with (Buffer B, 95:5 water/acetonitrile) with the modifiers 0.1% formic acid or 0.2% ammonium hydroxide with 50 mM ammonium acetate for positive and negative ionization mode, respectively. Each run used the following flow: 100% A at 0.2 mL/min for 5 min, followed by a gradient starting at 0% B linearly increasing to 100% B in 15 min with a flow rate of 0.7 mL/min, followed by an isocratic gradient of 100% B for 5 min at 0.7 mL/min before equilibrating for 5 min at 0% B with a flow rate of 0.7 mL/min. Metabolites were analyzed using the MassHunter software package (Agilent Technologies) by quantifying the SRM of the transition from precursor to product ions at associated collision energies and normalized to internal standard.

For neuraminidase treatment to release sialic acids from proteins and glycolipids, cell pellets (1×10^6 cells per replicate) were rinsed three times in PBS, soluble metabolites were extracted and removed with 40:40:20 acetonitrile/methanol/water, and the remaining precipitate was resuspended in 42 μL of PBS with 5 μL of 10× GlycoBuffer, and treated with 150 units of α-2,3,6,8-neuraminidase (New England BioLabs) overnight at 37 °C with shaking. Two hundred microliters of 1:1 acetonitrile:methanol was added the next day with inclusion of 10 nM d_3,^{15}N-serine, and 10 nM 2,3-^{13}C-*N*-acetylneuraminic acid as internal standards for extraction efficiency. Remaining insoluble debris was separated via centrifugation at 13 000 rpm for 10 min.

■ ASSOCIATED CONTENT

Ⓢ Supporting Information

The Supporting Information is available free of charge on the ACS Publications website at DOI: 10.1021/acschembio.6b00433.

Supplemental data including isotopic tracing, Western blot, and RNA sequencing (PDF)

Isotopic tracing of [^{13}C]glucose into metabolic pathways in an isogenic panel of MCF10A mammary epithelial cells individually expressing 11 oncogenes (XLSX)

Metabolomic profiling of ishCMAS 231MFP cells (XLSX)

Proteomic profiling of proteins enriched from ManNAz metabolic labeling of 231MFP cells (XLSX)

Transcriptional changes conferred by CMAS knockdown (XLSX)

■ AUTHOR INFORMATION

Corresponding Author

*E-mail: dnomura@berkeley.edu.

Notes

The authors declare no competing financial interest.

■ ACKNOWLEDGMENTS

This work was supported by grants from the National Institutes of Health (R01CA172667 for D.K.N., R.A.K., L.S.R.; U01MH105979 and U01HG007910 for N.Y.; NRSA Trainee appointment on grant number T32 for D.D.; R01CA170447 for A.G., U01CA168370 for S.B.), American Cancer Society Research Scholar Award (RSG14-242-01-TBE for D.K.N., R.A.K., L.S.R.), DOD Breakthroughs Award (CDMRP W81XWH-15-1-0050 for D.K.N., R.A.K., L.S.R.), the Searle Scholar Foundation (D.K.N., R.A.K., L.S.R.), the California

DOI: 10.1021/acschembio.6b00433
ACS Chem. Biol. XXXX, XXX, XXX−XXX

Research Alliance by BASF (CARA) (D.D., D.K.N.), DOD Era of Hope Award (CDMRP W81XWH-12-1-0272 for A.G.). The sequencing was carried out at the DNA Technologies and Expression Analysis Cores at the UC Davis Genome Center, supported by NIH Shared Instrumentation Grant 1S10OD010786-01.

REFERENCES

(1) Cantor, J. R., and Sabatini, D. M. (2012) Cancer cell metabolism: one hallmark, many faces. *Cancer Discovery 2*, 881−898.
(2) Pavlova, N. N., and Thompson, C. B. (2016) The Emerging Hallmarks of Cancer Metabolism. *Cell Metab. 23*, 27−47.
(3) Benjamin, D. I., Cravatt, B. F., and Nomura, D. K. (2012) Global profiling strategies for mapping dysregulated metabolic pathways in cancer. *Cell Metab. 16*, 565−577.
(4) Martins, M. M., Zhou, A. Y., Corella, A., Horiuchi, D., Yau, C., Rakshandehroo, T., Gordan, J. D., Levin, R. S., Johnson, J., Jascur, J., Shales, M., Sorrentino, A., Cheah, J., Clemons, P. A., Shamji, A. F., Schreiber, S. L., Krogan, N. J., Shokat, K. M., McCormick, F., Goga, A., and Bandyopadhyay, S. (2015) Linking tumor mutations to drug responses via a quantitative chemical-genetic interaction map. *Cancer Discovery 5*, 154−167.
(5) Büll, C., Stoel, M. A., den Brok, M. H., and Adema, G. J. (2014) Sialic acids sweeten a tumor's life. *Cancer Res. 74*, 3199−3204.
(6) Laughlin, S. T., and Bertozzi, C. R. (2007) Metabolic labeling of glycans with azido sugars and subsequent glycan-profiling and visualization via Staudinger ligation. *Nat. Protoc. 2*, 2930−2944.
(7) Nitschke, L., Floyd, H., and Crocker, P. R. (2001) New functions for the sialic acid-binding adhesion molecule CD22, a member of the growing family of Siglecs. *Scand. J. Immunol. 53*, 227−234.
(8) Jellusova, J., and Nitschke, L. (2012) Regulation of B cell functions by the sialic acid-binding receptors siglec-G and CD22. *Front. Immunol. 2*, Article No. 96.
(9) Cho, S., and Dawson, G. (2000) Palmitoyl protein thioesterase 1 protects against apoptosis mediated by Ras-Akt-caspase pathway in neuroblastoma cells. *J. Neurochem. 74*, 1478−1488.
(10) Cho, S., Dawson, P. E., and Dawson, G. (2000) Antisense palmitoyl protein thioesterase 1 (PPT1) treatment inhibits PPT1 activity and increases cell death in LA-N-5 neuroblastoma cells. *J. Neurosci. Res. 62*, 234−240.
(11) Koutsioumpa, M., and Papadimitriou, E. (2014) Cell surface nucleolin as a target for anti-cancer therapies. *Recent Pat. Anti-Cancer Drug Discovery 9*, 137−152.
(12) Benedetti, E., Antonosante, A., d'Angelo, M., Cristiano, L., Galzio, R., Destouches, D., Florio, T. M., Dhez, A. C., Astarita, C., Cinque, B., Fidoamore, A., Rosati, F., Cifone, M. G., Ippoliti, R., Giordano, A., Courty, J., and Cimini, A. (2015) Nucleolin antagonist triggers autophagic cell death in human glioblastoma primary cells and decreased in vivo tumor growth in orthotopic brain tumor model. *Oncotarget 6*, 42091−42104.
(13) Dhawan, P., and Richmond, A. (2002) Role of CXCL1 in tumorigenesis of melanoma. *J. Leukoc. Biol. 72*, 9−18.
(14) Heo, S.-H., Lee, J.-Y., Yang, K.-M., and Park, K.-S. (2015) ELK3 Expression Correlates With Cell Migration, Invasion, and Membrane Type 1-Matrix Metalloproteinase Expression in MDA-MB-231 Breast Cancer Cells. *Gene Expression 16*, 197−203.
(15) Lee, Y.-K., Lee, S.-Y., Park, J.-R., Kim, R.-J., Kim, S.-R., Roh, K.-J., and Nam, J.-S. (2012) Dysadherin expression promotes the motility and survival of human breast cancer cells by AKT activation. *Cancer Sci. 103*, 1280−1289.
(16) Jakowlew, S. B. (2006) Transforming growth factor-beta in cancer and metastasis. *Cancer Metastasis Rev. 25*, 435−457.
(17) Su, M.-L., Chang, T.-M., Chiang, C.-H., Chang, H.-C., Hou, M.-F., Li, W.-S., and Hung, W.-C. (2014) Inhibition of chemokine (C-C motif) receptor 7 sialylation suppresses CCL19-stimulated proliferation, invasion and anti-anoikis. *PLoS One 9*, e98823.
(18) Hauser, M. A., Kindinger, I., Laufer, J. M., Späte, A.-K., Bucher, D., Vanes, S. L., Krueger, W. A., Wittmann, V., and Legler, D. F. (2016) Distinct CCR7 glycosylation pattern shapes receptor signaling and endocytosis to modulate chemotactic responses. *J. Leukocyte Biol. 99*, 993.
(19) Sperandio, M. (2012) The expanding role of α2−3 sialylation for leukocyte trafficking in vivo. *Ann. N. Y. Acad. Sci. 1253*, 201−205.
(20) Miller, L. J., Kurtzman, S. H., Anderson, K., Wang, Y., Stankus, M., Renna, M., Lindquist, R., Barrows, G., and Kreutzer, D. L. (2000) Interleukin-1 family expression in human breast cancer: interleukin-1 receptor antagonist. *Cancer Invest. 18*, 293−302.
(21) Knüpfer, H., and Preiss, R. (2007) Significance of interleukin-6 (IL-6) in breast cancer (review). *Breast Cancer Res. Treat. 102*, 129−135.
(22) Goldberg, J. E., and Schwertfeger, K. L. (2010) Proinflammatory cytokines in breast cancer: mechanisms of action and potential targets for therapeutics. *Curr. Drug Targets 11*, 1133−1146.
(23) Balkwill, F. (2004) Cancer and the chemokine network. *Nat. Rev. Cancer 4*, 540−550.
(24) Lucena, M. C., Carvalho-Cruz, P., Donadio, J. L., Oliveira, I. A., de Queiroz, R. M., Marinho-Carvalho, M. M., Sola-Penna, M., de Paula, I. F., Gondim, K. C., McComb, M. E., Costello, C. E., Whelan, S. A., Todeschini, A. R., and Dias, W. B. (2016) Epithelial mesenchymal transition induces aberrant glycosylation through hexosamine biosynthetic pathway activation. *J. Biol. Chem. 291*, 12917.
(25) Ying, H., Kimmelman, A. C., Lyssiotis, C. A., Hua, S., Chu, G. C., Fletcher-Sananikone, E., Locasale, J. W., Son, J., Zhang, H., Coloff, J. L., Yan, H., Wang, W., Chen, S., Viale, A., Zheng, H., Paik, J., Lim, C., Guimaraes, A. R., Martin, E. S., Chang, J., Hezel, A. F., Perry, S. R., Hu, J., Gan, B., Xiao, Y., Asara, J. M., Weissleder, R., Wang, Y. A., Chin, L., Cantley, L. C., and DePinho, R. A. (2012) Oncogenic Kras Maintains Pancreatic Tumors through Regulation of Anabolic Glucose Metabolism. *Cell 149*, 656−670.
(26) Tamura, F., Sato, Y., Hirakawa, M., Yoshida, M., Ono, M., Osuga, T., Okagawa, Y., Uemura, N., Arihara, Y., Murase, K., Kawano, Y., Iyama, S., Takada, K., Hayashi, T., Sato, T., Miyanishi, K., Kobune, M., Takimoto, R., and Kato, J. (2016) RNAi-mediated gene silencing of ST6GalNAc I suppresses the metastatic potential in gastric cancer cells. *Gastric Cancer 19*, 85−97.
(27) Wellen, K. E., Lu, C., Mancuso, A., Lemons, J. M. S., Ryczko, M., Dennis, J. W., Rabinowitz, J. D., Coller, H. A., and Thompson, C. B. (2010) The hexosamine biosynthetic pathway couples growth factor-induced glutamine uptake to glucose metabolism. *Genes Dev. 24*, 2784−2799.
(28) Jóźwiak, P., Forma, E., Bryś, M., and Krześlak, A. (2014) O-GlcNAcylation and Metabolic Reprograming in Cancer. *Front. Endocrinol. 5*, ArticleNo. 145.
(29) Kohnz, R. A., Mulvihill, M. M., Chang, J. W., Hsu, K.-L., Sorrentino, A., Cravatt, B. F., Bandyopadhyay, S., Goga, A., and Nomura, D. K. (2015) Activity-Based Protein Profiling of Oncogene-Driven Changes in Metabolism Reveals Broad Dysregulation of PAFAH1B2 and 1B3 in Cancer. *ACS Chem. Biol. 10*, 1624−1630.
(30) Campeau, E. (2009) A Versatile Viral System for Expression and Depletion of Proteins in Mammalian Cells. *PLoS ONE 4*, e6529.
(31) Medina-Cleghorn, D., Bateman, L. A., Ford, B., Heslin, A., Fisher, K. J., Dalvie, E. D., and Nomura, D. K. (2015) Mapping Proteome-Wide Targets of Environmental Chemicals Using Reactivity-Based Chemoproteomic Platforms. *Chem. Biol. 22*, 1394−1405.
(32) Bolger, A. M., Lohse, M., and Usadel, B. (2014) Trimmomatic: a flexible trimmer for Illumina sequence data. *Bioinformatics 30*, 2114−2120.
(33) Langmead, B., and Salzberg, S. L. (2012) Fast gapped-read alignment with Bowtie 2. *Nat. Methods 9*, 357−359.
(34) Li, B., and Dewey, C. N. (2011) RSEM: accurate transcript quantification from RNA-Seq data with or without a reference genome. *BMC Bioinf. 12*, 323.
(35) Love, M. I., Huber, W., and Anders, S. (2014) Moderated estimation of fold change and dispersion for RNA-seq data with DESeq2. *Genome Biol. 15*, 550.

DOI: 10.1021/acschembio.6b00433
ACS Chem. Biol. XXXX, XXX, XXX−XXX

(36) Benjamini, Y., and Hochberg, Y. (1995) Controlling the False Discovery Rate: A Practical and Powerful Approach to Multiple Testing. *J. R. Stat. Soc. Ser. B Methodol. 57*, 289−300.

DOI: 10.1021/acschembio.6b00433
ACS Chem. Biol. XXXX, XXX, XXX−XXX